


High-pressure order-disorder transition in Mg_2SiO_4 : Implications for super-Earth mineralogy

Rajkrishna Dutta ^{1,2,*}, Sally J. Tracy,¹ and R. E. Cohen¹

¹*Earth and Planets Laboratory, Carnegie Institution for Science, Washington, DC 20015, USA*

²*Discipline of Earth Sciences, Indian Institute of Technology Gandhinagar, Gujarat 382355, India*



(Received 13 February 2023; accepted 2 May 2023; published 22 May 2023)

(Mg, Fe) SiO_3 post-perovskite is the highest-pressure silicate mineral phase in the Earth's interior. The extreme pressure and temperature conditions inside large extrasolar planets will likely lead to phase transitions beyond post-perovskite. In this work, we have explored the high-pressure phase relations in Mg_2SiO_4 using computations based on density functional theory. We find that a partially disordered $I\bar{4}2d$ -type structure would be stable under the conditions expected for the interiors of super-Earth planets. We have explored the mechanism of the phase transition from the ordered ground state and the effect of disordering on the electronic properties of the silicate phase. The discovery of a structure where two very dissimilar cations, Mg^{2+} and Si^{4+} , occupy the same crystallographic site opens up a domain of interesting crystal chemistry and provides a foundation for other silicates and oxides with mixed occupancy.

DOI: [10.1103/PhysRevB.107.184112](https://doi.org/10.1103/PhysRevB.107.184112)

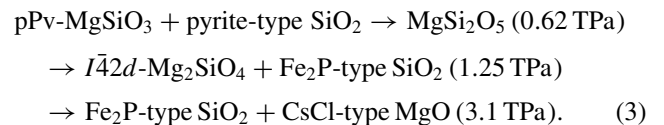
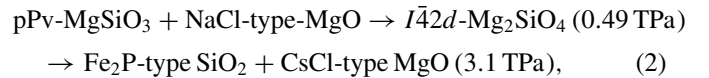
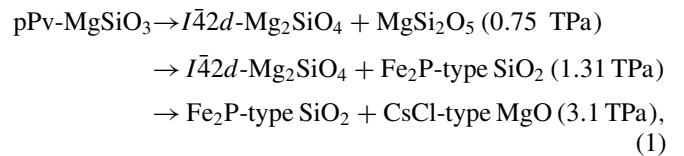
I. INTRODUCTION

The lower mantle of the Earth is believed to be primarily composed of (Mg, Fe) SiO_3 perovskite (bridgmanite, Pv) [1]. With increasing pressure and temperature, magnesium-rich bridgmanite transforms to a layered CaIrO_3 -type structure called post-perovskite (pPv) [2]. The properties of the pPv phase offer a probable explanation for several unusual properties (e.g., seismic anisotropy, topography, and geochemical anomalies) of the D'' -layer [3] at the base of the lower mantle. No further phase transitions are expected in the Earth. Recent advances in astronomy and planetary sciences have led to the discovery of many exoplanets. To date, more than 5200 exoplanets [4] have been confirmed, of which >1500 are super-Earth planets ($M_E < M < 10M_E$). Super-Earth planets with a rocky interior are particularly significant because of their potential to harbor life. The mantles of these terrestrial exoplanets are likely made of earth-forming silicate minerals with a range (0.67–1.5) of Mg/Si ratios [5,6]. The extreme pressure and temperature conditions (Fig. 1) inside these planets are expected to stabilize phases beyond post-perovskite. Knowledge of these phase transitions is crucial to understanding the dynamics and evolution of these planetary interiors.

The ultrahigh-pressure phase relations in the MgO-SiO₂ system have been extensively studied both experimentally and computationally. Laser-heated diamond cell experiments on Mg_2SiO_4 suggest MgSiO_3 pPv remains stable at least up to 265 GPa [7]. Higher pressure-temperature conditions remain inaccessible for even state-of-the-art static compression techniques. Shock melting has been reported to occur at ~ 250 GPa for Mg_2SiO_4 [8], while MgSiO_3 glass melts at 180 GPa along the Hugoniot [9]. Studies using bridgmanite starting material [6,10] observe shock melt-

ing at ~ 500 GPa. However, none of these experiments have reported a direct observation of pPv or any post-pPv phases.

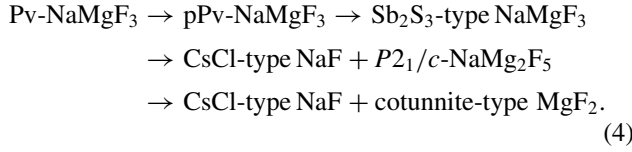
Due to the challenges in accessing these extreme pressure and temperature conditions, our understanding of the mineralogy of terrestrial exoplanets is largely based on quantum-mechanical computations. Computational studies [11–15] suggest pPv MgSiO_3 would ultimately dissociate into an assemblage of binary oxides after two or three stages of partial dissociation as follows:



$I\bar{4}2d$ -type Mg_2SiO_4 was found computationally in compositions with a wide range of Mg/Si ratios [15]. Our recent experiments have explored the stability of this type of structure in NaMgF_3 [16] and Mg_2GeO_4 [17], well-known analogs [18] of the MgO-SiO₂ system. The tetragonal $I\bar{4}2d$ -type phase has not been experimentally observed in either case. In NaMgF_3 , our experiments found the following transition

*Corresponding author: raj.dutta@iitgn.ac.in

sequence:



Mg_2GeO_4 , on the other hand, was found to be stable in the thorium phosphide ($I\bar{4}3d$) structure or a disordered tetragonal $I\bar{4}2d$ phase, experimentally indistinguishable from the $I\bar{4}3d$ structure at pressures above ~ 175 GPa. In this study, we have explored the stability and nature of the $I\bar{4}2d$ - and $I\bar{4}3d$ -type phases in Mg_2SiO_4 using density functional theory (DFT) computations.

II. COMPUTATIONAL DETAILS

We have performed plane-wave density functional theory computations as implemented in the QUANTUM ESPRESSO [19] package. All computations were performed with the PBE exchange correlation functional and GBRV potentials [20]. An energy cutoff of 40 Ry was used for the orbitals. The Brillouin zone for the pPv and the ordered $I\bar{4}2d$ -type structures were sampled with a $6 \times 6 \times 6$ k -point grid.

To understand the behavior of the order-disorder transition, we considered an order parameter, Q . The order parameter was varied from 0 (completely disordered) to 1 (completely ordered) with 11 intermediate values using the following relation: $X_{\text{Mg}}(8d) = -Q \times 1/3 + 2/3$ and $X_{\text{Mg}}(4a) = -Q \times 2/3 + 2/3$. The disordered structures were generated using the ATAT toolkit [21] following the Special Quasirandom Structure method [22,23]. For each Q , we generated a 224-atom ($2 \times 2 \times 2$) supercell with the lattice parameters of the cubic disordered phase doubled in each direction. For each supercell, the objective function that attempts to match the maximum number of correlation functions of the SQS structure and the disordered state is calculated considering clusters of two cation pairs up to 5.0 Å. The objective function is then minimized using a Monte Carlo method. The best (lowest objective function) SQS structure was then optimized at the required pressure by relaxing both lattice parameters and atomic positions using the Broyden-Fletcher-Goldfarb-Shanno algorithm until the forces were $< 5 \times 10^{-4}$ Ry/Bohr. All relaxations were carried out at the Γ point with a 40 Ry energy cutoff. To test the convergence of the calculations, we also performed a couple of optimizations with different k -point grids and energy cutoffs (Table S1 of the Supplemental Material [24]). The same exercise was repeated for 13 configurations of the order parameter from $Q = 0$ ($I\bar{4}3d$) to 1 ($I\bar{4}2d$). The variation in enthalpy with Q could be well-fitted with a second-degree polynomial; no higher-order fits were necessary. The disordering enthalpy (H) is counteracted by the configurational entropy ($\frac{S}{k_B} = -\sum X \ln X$), where the sum is over the sites, X is the mole fraction of Mg or Si on each site, and k_B is the Boltzmann constant. The free energy ($H - TS$) is minimized at each temperature to obtain the variation in Q with temperature. A MATHEMATICA [25] script, sample input file, and instructions for this calculation have been provided in the Supplemental Material [24]. For the density of state (DOS) computations, a finer $4 \times 4 \times 4$ k -point grid was used.

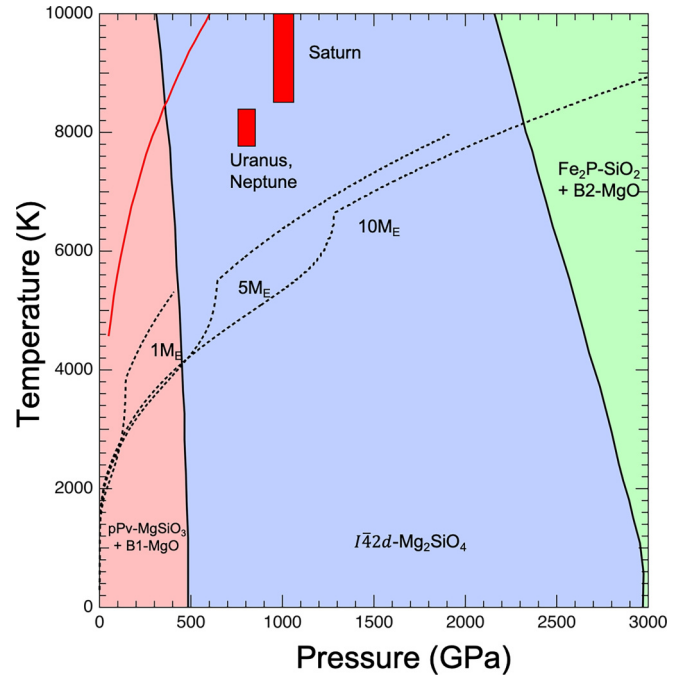


FIG. 1. Theoretically computed phase boundaries (solid black lines) in the Mg_2SiO_4 system [15]. Dashed black lines show the pressure and temperature conditions inside terrestrial exoplanets [29] with masses equal to 5 and 10 times that of the Earth (M_E). Solid red line shows the melting curve of MgSiO_3 [6]. Red rectangles indicate estimated core-envelope P and T conditions in giant planets in the solar system.

III. RESULTS

Initially, we optimized the structures of $I\bar{4}2d$ -type Mg_2SiO_4 , pPv MgSiO_3 , and MgO (B1,B2) at select pressures. The structure of post-perovskite MgSiO_3 (space group: $CmCm$) consists of edge and corner sharing silicate octahedra (coordination number, $CN = 6$) forming layers along the b -axis. B1 ($Fm\bar{3}m$) and B2 ($Pm\bar{3}m$) MgO have the sixfold-coordinated rocksalt and CsCl-type structures, respectively. In agreement with existing experiments [26] and *ab initio* calculations [27], we find that B1- MgO transforms into B2- MgO at 525 GPa. Post-perovskite $\text{MgSiO}_3 + \text{MgO}$ (B1/B2) is found to recombine into $I\bar{4}2d$ -type Mg_2SiO_4 at 535/545 GPa (Fig. 2). Considering the different functional (PBE) used in this study, this is in reasonable agreement with Umemoto *et al.* [15] (490 GPa using the local density approximation). The reaction line to form $I\bar{4}2d$ -type Mg_2SiO_4 has a negative Clapeyron slope (-16 MPa/K) at the pressure and temperature conditions [15] expected in super-Earth mantles. $I\bar{4}2d$ -type Mg_2SiO_4 has a body-centered-tetragonal structure with two different cation sites: Mg ($8d$) and Si ($4a$). Both Mg and Si show eightfold coordination. The ordered $I\bar{4}2d$ -type structure was not observed experimentally in Mg_2GeO_4 [17], a widely used analog of Mg_2SiO_4 . Instead, an intrinsically disordered $I\bar{4}3d$ -type or a highly disordered $I\bar{4}2d$ -type structure was found to be stable at pressures > 175 GPa. Recent studies on Mg_2GeO_4 [17,27] show that the $I\bar{4}3d$ phase can be understood in terms of an order-disorder transition from the $I\bar{4}2d$ structure. In the $I\bar{4}3d$ -type structure, the Mg and Si

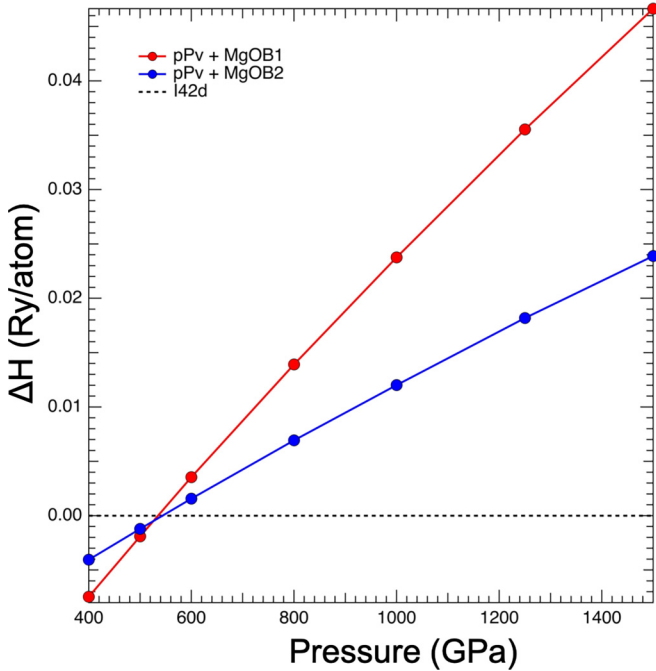


FIG. 2. Enthalpy differences (ΔH) between post-perovskite $\text{MgSiO}_3 + \text{MgO}$ (B1/B2) and $I\bar{4}2d$ -type Mg_2SiO_4 as a function of pressure for the static lattice (classical 0 K). The dashed black line indicates $\Delta H = 0$; the crossover with the respective phases shows the transition pressure.

coordination remains unchanged, but the cations occupy a single site ($12a$; Mg: 2/3, Ge: 1/3).

Figure 3 shows the structure (224-atom supercell) of partially disordered ($Q = 0.53$) and completely disordered Mg_2SiO_4 . The nature and order of the transition [29] are dependent on the behavior of enthalpy, $H(Q)$, in comparison to entropy, $S(Q)$. The order parameter can abruptly change with temperature (first order) or show a continuous change. Figures 4(a) and 4(b) show the change in enthalpy and entropy as a function of the order parameter, respectively, at 600, 800, and 1500 GPa. The enthalpy of disorder increases by 0.012, 0.014, and 0.018 Ry/atom at 600, 800, and 1500 GPa, respectively, on complete disordering ($Q = 1 \rightarrow Q = 0$). The configurational entropy (p.f.u.) is zero in the completely ordered $I\bar{4}2d$ structure and 1.9095 in the completely disordered $I\bar{4}3d$ structure.

Figure 5 shows the change in the order parameter with temperature. Q is found to vary smoothly with temperature, suggesting a gradual disordering with temperature. At 600 GPa, disordering is found to start at 1100 K ($Q = 0.999$), with a continuous decrease in Q to the peak temperature of 20 000 K ($Q = 0.056$). At higher pressures, the amount of disorder is less at a particular temperature, suggesting a positive Clapeyron slope between the ordered and disordered structures. This is in agreement with the transition slope reported in Mg_2GeO_4 [28]. In this case, the transition is isostructural within the $I\bar{4}2d$ space group, from a highly ordered to a moderately disordered structure. The ordering is convergent because the two cation sites in the tetragonal structure eventually becomes equivalent leading to a change in symmetry (cubic). The disordering

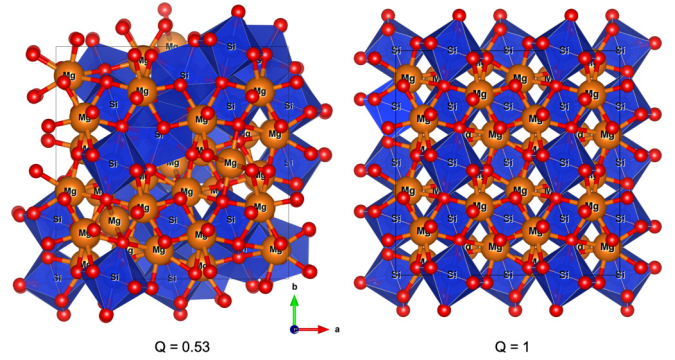


FIG. 3. Crystal structure (224-atom supercell) of partially and completely ordered $I\bar{4}2d$ -type Mg_2SiO_4 at 600 GPa.

process becomes sluggish at high Q values, as can be seen from the nearly horizontal slope at $Q < 0.15$. This can be explained using the relative changes in enthalpy of disorder and configurational entropy. The ΔS ordering is fairly flat [Fig. 4(b)] from $Q = 0.2$ to 0, whereas ΔH continues to increase [Fig. 4(b)], so it does not pay to order completely, even at extremely high temperatures ($> 20\,000$ K).

Figures 6(a) and 6(b) show the change in unit-cell volume and the c/a ratio as a function of the order parameter. Disorder does not have a significant effect on the cell volume, showing a 0.6%, 0.5%, and 0.3% decrease over the entire Q range at 600, 800, and 1500 GPa, respectively. The c/a ratio changes from 1 in the cubic phase to 1.036, 1.030, and 1.022, respectively, in the completely ordered tetragonal structure.

At pressure and temperature conditions relevant to the interior of giant super-Earth planets, the mineral phases are expected to be semiconductors with band gaps [11]. Figure S1 of the Supplemental Material [24] shows the DFT computed electronic band gap of Mg_2SiO_4 as a function of pressure and order parameter. Figure S2 shows the density of states (DOS) of the completely ordered and completely disordered $I\bar{4}2d$ -type structure at 800 GPa. Increase in pressure leads to a slight increase in the band gap with pressure at a given Q (Fig. S3). Disorder, on the other hand, has a significant effect on the electronic structure of Mg_2SiO_4 . The peak values of the DOS in both the valence and conduction bands decrease from $Q = 1$ to 0, suggesting an increase in the overlap of the bonds. The calculated band gaps (which probably grossly underestimate the true gaps) of the completely ordered $I\bar{4}2d$ -type phase are 10.44, 10.74, and 10.89 eV at 600, 800, and 1500 GPa, respectively. This is significantly higher than the reported values for MgSiO_3 and the binary oxides at the respective pressures. A complete disorder of the silicate would lead to a $\sim 61\%$ reduction in the band gap at considered pressures.

IV. DISCUSSION AND CONCLUSION

In this study, we have shown that MgSiO_3 post-perovskite+MgO will recombine into $I\bar{4}2d$ -type Mg_2SiO_4 at pressures > 535 GPa. Our computations suggest that the ordered tetragonal $I\bar{4}2d$ -type structure will gradually disorder with increasing temperature. For a terrestrial super-Earth with mass equal to $10M_E$, the pressure and temperature at

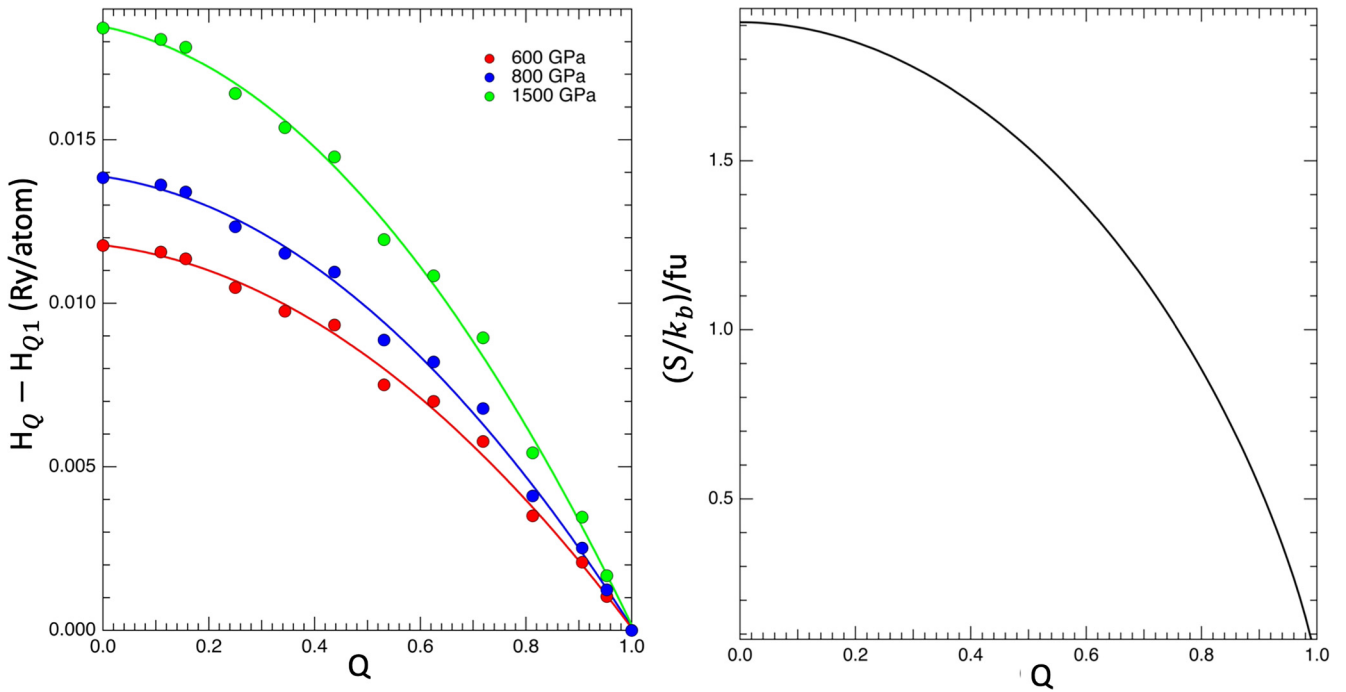


FIG. 4. Difference in enthalpy ($H_Q - H_{Q1}$) (left) vs order parameter Q at 600, 800, and 1500 GPa, where H_{Q1} is the enthalpy of the completely ordered phase ($Q = 1$). Configurational entropy at 600 GPa (right).

the core-mantle boundary are likely to be ~ 1300 GPa and 6500 K [30], while the melting point of MgSiO_3 is expected to be $\sim 13\,000$ K at 1500 GPa. Thus, a complete disorder into

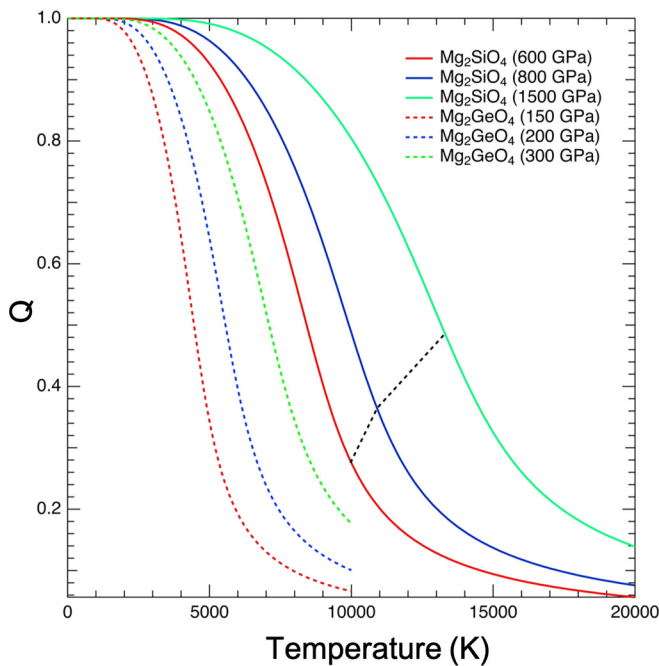


FIG. 5. Change in the order parameter Q with temperature for $I\bar{4}2d$ -type Mg_2SiO_4 (solid) and Mg_2GeO_4 (dashed) [17] at select pressures. $Q = 0$ and 1 correspond to completely disordered and completely ordered structures, respectively. Black dotted line shows the predicted melting temperature [6] of MgSiO_3 based on extrapolation of shockwave melting data.

the cubic $I\bar{4}3d$ -type structure is not expected at conditions relevant to planetary interiors; instead, a partially disordered $I\bar{4}2d$ -type Mg_2SiO_4 is potentially the stable silicate phase.

In a recent work [17], we explored the high-pressure behavior of Mg_2GeO_4 , a very good analog for Mg_2SiO_4 . The germanate mirrors the phase-transition sequence [2,31] in the silicate ($\text{Pv} \rightarrow \text{pPv}$ at 125 GPa, $\text{pPv} + \text{MgO} \rightarrow \text{Mg}_2\text{GeO}_4$ at 535 GPa), but at substantially lower pressures ($\text{Pv} \rightarrow \text{pPv}$ at 65 GPa, $\text{pPv} + \text{MgO} \rightarrow \text{Mg}_2\text{GeO}_4$ at ~ 185 GPa). Figure 5 compares the change in order parameter with temperature in Mg_2SiO_4 and Mg_2GeO_4 . The computationally predicted ground-state structure, i.e., the ordered $I\bar{4}2d$ -type structure, was not experimentally observed in the germanate. Instead, a disordered $I\bar{4}3d$ -type or a highly disordered ($Q > 0.53$) $I\bar{4}2d$ -type structure, experimentally indistinguishable (i.e., the peak splittings expected for the tetragonal structure cannot be experimentally resolved) from the completely disordered Th_3P_4 -type structure, was found to be consistent with the x-ray diffraction patterns. Mg_2SiO_4 , on the other hand, is expected to disorder less at pressures close to the $\text{pPv} + \text{MgO} \rightarrow I\bar{4}2d$ transition.

The perovskite to post-perovskite phase transition in MgSiO_3 is accompanied by a 1–1.5 % reduction in volume [32]. The post-post-perovskite transition to the partially disordered $I\bar{4}2d$ -type structure is computed to have a 0.8–1.4 % (depending on degree of disorder) change in volume at 600 GPa. The large negative Clapeyron slope [15] of the transition combined with a modest volume change can lead to a possible boundary layer in the super-Earth mantles.

The Th_3P_4 -type or modified $I\bar{4}2d$ structure is common in A_2X_3 , A_3X_4 , and AB_2X_4 rare-earth chalcogenides [33,34].

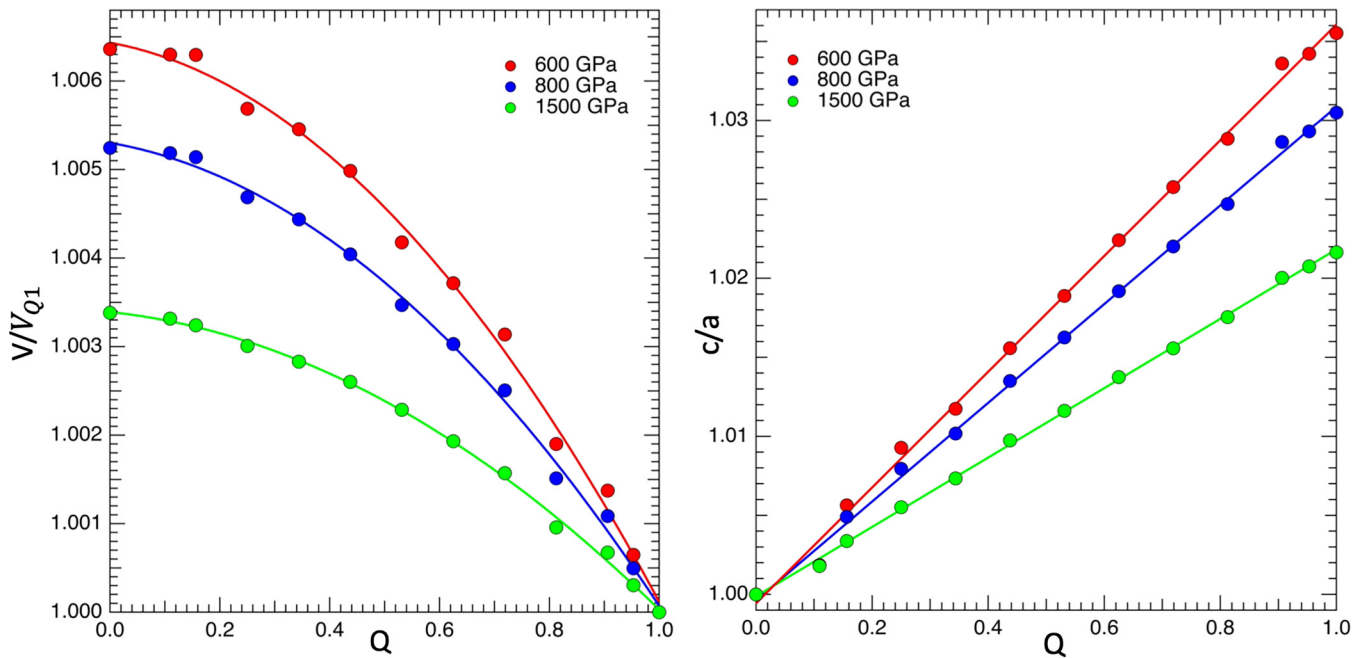


FIG. 6. Variation in unit-cell volume (left) and c/a (right) of $I42d$ -type Mg_2SiO_4 as a function of the order parameter Q at 600, 800, and 1500 GPa.

The structure has found widespread technical applications because it is highly flexible and can incorporate defects and impurities [35]. A recent study also reported a modified Th_3P_4 -type structure in Fe_3O_4 at 78 GPa and 4800 K [36,37]. The structural flexibility and widespread occurrence of this structure in chalcogenides, oxides, and silicates/germanates make it a possible important transition pathway. The intrinsically disordered nature of this phase has important implications for chemical miscibility at

high P - T conditions, and may lead to anomalous thermal conductivities.

ACKNOWLEDGMENTS

R.D. gratefully acknowledges support from the Carnegie Endowment and IIT Gandhinagar. Computations were performed using the GCS Supercomputer SuperMUC-NG at Leibniz Supercomputing Centre (LRZ).

- [1] O. Tschauner, C. Ma, J. R. Beckett, C. Prescher, V. B. Prakapenka, and G. R. Rossman, Discovery of bridgmanite, the most abundant mineral in earth, in a shocked meteorite, *Science* **346**, 1100 (2014).
- [2] M. Murakami, K. Hirose, K. Kawamura, N. Sata, and Y. Ohishi, Post-perovskite phase transition in $MgSiO_3$, *Science* **304**, 855 (2004).
- [3] A. R. Oganov, R. Martoňák, A. Laio, P. Raiteri, and M. Parrinello, Anisotropy of earth's D'' layer and stacking faults in the $MgSiO_3$ post-perovskite phase, *Nature (London)* **438**, 1142 (2005).
- [4] NASA Exoplanet Catalog, <https://exoplanets.nasa.gov/discovery/exoplanet-catalog/>.
- [5] F. D. Albareti *et al.*, The 13th data release of the sloan digital sky survey: First spectroscopic data from the SDSS-IV survey mapping nearby galaxies at apache point observatory, *Astrophys. J.* **233**, 25 (2017).
- [6] Y. Fei, C. T. Seagle, J. P. Townsend, C. A. McCoy, A. Boujibar, P. Driscoll, L. Shulenburger, and M. D. Furnish, Melting and density of $MgSiO_3$ determined by shock compression of bridgmanite to 1254 GPa, *Nat. Commun* **12**, 876 (2021).
- [7] T. Sakai, H. Dekura, and N. Hirao, Experimental and theoretical thermal equations of state of $MgSiO_3$ post-perovskite at multi-megabar pressures, *Sci. Rep.* **6**, 22652 (2016).
- [8] J. M. Brown, M. D. Furnish, and R. G. McQueen, Thermodynamics for $(Mg, Fe)_2SiO_4$ from the Hugoniot, in *High-Pressure Research in Mineral Physics: A Volume in Honor of Syun-Iti Akimoto AGU, 1987*, Vol. 39 (Wiley, 1987), pp. 373–384.
- [9] J. L. Mosenfelder, P. D. Asimow, D. J. Frost, D. C. Rubie, and T. J. Ahrens, The $MgSiO_3$ system at high pressure: thermodynamic properties of perovskite, postperovskite, and melt from global inversion of shock and static compression data, *J. Geophys. Res.* **114**, B01203 (2009).
- [10] M. Millot, S. Zhang, D. E. Fratanduono, F. Coppari, S. Hamel, B. Militzer, D. Simonova, S. Shcheka, N. Dubrovinskaia, L. Dubrovinsky, and J. H. Eggert, Recreating giants impacts in the laboratory: shock compression of $MgSiO_3$ bridgmanite to 14 Mbar, *Geophys. Res. Lett.* **47**, e2019GL085476 (2020).
- [11] K. Umemoto, R. M. Wentzcovitch, and P. B. Allen, Dissociation of $MgSiO_3$ in the cores of gas giants and terrestrial exoplanets, *Science* **311**, 983 (2006).

- [12] K. Umemoto and R. M. Wentzcovitch, Two-stage dissociation in MgSiO_3 post-perovskite, *Earth Planet. Sci. Lett.* **311**, 225 (2011).
- [13] S. Q. Wu, M. Ji, C. Z. Wang, M. C. Nguyen, X. Zhao, K. Umemoto, R. M. Wentzcovitch, and K. M. Ho, An adaptive genetic algorithm for crystal structure prediction, *J. Phys.: Condens. Matter* **26**, 035402 (2013).
- [14] H. Niu, A. R. Oganov, X.-Q. Chen, and D. Li, Prediction of novel stable compounds in the Mg-Si-O system under exoplanet pressures, *Sci. Rep.* **5**, 18347 (2015).
- [15] K. Umemoto, R. M. Wentzcovitch, S. Wu, M. Ji, C.-Z. Wang, and K.-M. Ho, Phase transitions in MgSiO_3 post-perovskite in super-earth mantles, *Earth Planet. Sci. Lett.* **478**, 40 (2017).
- [16] R. Dutta, E. Greenberg, V. B. Prakapenka, and T. S. Duffy, Phase transitions beyond post-perovskite in NaMgF_3 to 160 GPa, *Proc. Natl. Acad. Sci. (USA)* **116**, 19324 (2019).
- [17] R. Dutta *et al.*, Ultrahigh-pressure disordered eight-coordinated phase of Mg_2GeO_4 : Analogue for super-earth mantles, *Proc. Natl. Acad. Sci. (USA)* **119**, e2114424119 (2022).
- [18] C. V. Stan, R. Dutta, R. J. Cava, V. B. Prakapenka, and T. S. Duffy, High-pressure study of perovskites and postperovskites in the (Mg,Fe)GeO₃ system, *Inorg. Chem.* **56**, 8026 (2017).
- [19] P. Giannozzi, S. Baroni, N. Bonini, M. Calandra, R. Car, C. Cavazzoni, D. Ceresoli, G. L. Chiarotti, M. Cococcioni, I. Dabo, A. Dal Corso, S. Fabris, G. Fratesi, S. de Gironcoli, R. Gebauer, U. Gerstmann, C. Gougoussis, A. Kokalj, M. Lazzeri, L. Martin-Samos, N. Marzari, F. Mauri, R. Mazzarello, S. Paolini, A. Pasquarello, L. Paulatto, C. Sbraccia, S. Scandolo, G. Sclauzero, A. P. Seitsonen, A. Smogunov, P. Umari, and R. M. Wentzcovitch, *J. Phys.: Condens. Matter* **21**, 395502 (2009).
- [20] K. F. Garrity, J. W. Bennett, K. M. Rabe, and D. Vanderbilt, Pseudopotentials for high-throughput DFT calculations, *Comput. Mater. Sci.* **81**, 446 (2014).
- [21] A. van de Walle, P. Tiwary, M. de Jong, D. L. Olmsted, M. Asta, A. Dick, D. Shin, Y. Wang, L.-Q. Chen, and Z.-K. Liu, Efficient stochastic generation of special quasirandom structures, *Calphad* **42**, 13 (2013).
- [22] S.-H. Wei, L. G. Ferreira, J. E. Bernard, and A. Zunger, Electronic properties of random alloys: Special quasirandom structures, *Phys. Rev. B* **42**, 9622 (1990).
- [23] A. Zunger, S.-H. Wei, L. G. Ferreira, and J. E. Bernard, Special Quasirandom Structures, *Phys. Rev. Lett.* **65**, 353 (1990).
- [24] See Supplemental Material at <http://link.aps.org/supplemental/10.1103/PhysRevB.107.184112> for the convergence criterion, band structure and density of states.
- [25] Wolfram, Research. Inc, Mathematica (2021), <https://istf.iitgn.ac.in/software/>.
- [26] F. Coppari, R. F. Smith, J. H. Eggert, J. Wang, J. R. Rygg, A. Lazicki, J. A. Hawreliak, G. W. Collins, and T. S. Duffy, Experimental evidence for a phase transition in magnesium oxide at exoplanet pressures, *Nat. Geosci.* **6**, 926 (2013).
- [27] M. J. Mehl, R. E. Cohen, and H. Krakauer, Linearized augmented plane wave electronic structure calculations for MgO and CaO, *J. Geophys. Res.: Solid Earth* **93**, 8009 (1988).
- [28] K. Umemoto and R. M. Wentzcovitch, Ab initio prediction of an order-disorder transition in Mg_2GeO_4 : Implication for the nature of super-earth's mantles, *Phys. Rev. Mater.* **5**, 093604 (2021).
- [29] T. Holland and R. Powell, Thermodynamics of order-disorder in minerals; I, symmetric formalism applied to minerals of fixed composition, *Am. Miner.* **81**, 1413 (1996).
- [30] F. W. Wagner, N. Tosi, F. Sohl, H. Rauer, and T. Spohn, Rocky super-earth interiors - structure and internal dynamics of CoRoT-7b and Kepler-10b, *Astron. Astrophys.* **541**, A103 (2012).
- [31] K. Hirose, K. Kawamura, Y. Ohishi, S. Tateno, and N. Sata, Stability and equation of state of MgGeO_3 post-perovskite phase, *Am. Mineral* **90**, 262 (2005).
- [32] K. Hirose, Postperovskite phase transition and its geophysical implications, *Rev. Geophys.* **44**, RG3001 (2006).
- [33] J. Flahaut, M. Guittard, M. Patrie, M. P. Pardo, S. M. Golabi, and L. Domange, Phase cubiques type Th_3P_4 dans les sulfures, les sélénures et les tellures L_2X_3 et L_3X_4 des terres rares, et dans leurs combinaisons ML_2X_4 avec les sulfures et sélénures MX de calcium, strontium et baryum. Formation et propriétés cristallines, *Acta Cryst.* **19**, 14 (1965).
- [34] X. Zhang and A. Zunger, Diagrammatic separation of different crystal structures of A_2BX_4 compounds without energy minimization: A pseudopotential orbital radii approach, *Adv. Funct. Mater.* **20**, 1944 (2010).
- [35] C. E. Whiting, E. S. Vasquez, and C. D. Barklay, Uranium based materials as potential thermoelectric couples for future radioisotope power systems, in *2018 IEEE Aerospace Conference* (IEEE, Piscataway, NJ, 2018), pp. 1–9.
- [36] S. Khandarkhaeva, T. Fedotenko, S. Chariton, E. Bykova, S. V. Ovsyannikov, K. Glazyrin, H.-P. Liermann, V. Prakapenka, N. Dubrovinskaia, and L. Dubrovinsky, Structural diversity of magnetite and products of its decomposition at extreme conditions, *Inorg. Chem.* **61**, 1091 (2022).
- [37] C. C. Zurkowski, J. Yang, S. Chariton, V. B. Prakapenka, and Y. Fei, Synthesis and stability of an eight-coordinated Fe_3O_4 high-pressure phase: Implications for the mantle structure of super-earths, *J. Geophys. Res.: Planets* **127**, e2022JE007344 (2022).